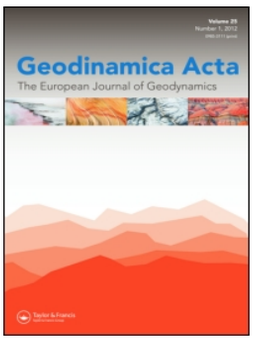

Geodinamica Acta

ISSN: 0985-3111 (Print) 1778-3593 (Online) Journal homepage: https://www.tandfonline.com/loi/tgda20

Geochemical constraints on provenance and source area weathering of metasedimentary rocks from the Paleoproterozoic (~2.1 Ga) Wa-Lawra Belt, southeastern margin of the West African Craton

Daniel K. Asiedu, Magdalene Agoe, Prince O. Amponsah, Prosper M. Nude & Chris Y. Anani

To cite this article: Daniel K. Asiedu, Magdalene Agoe, Prince O. Amponsah, Prosper M. Nude & Chris Y. Anani (2019) Geochemical constraints on provenance and source area weathering of metasedimentary rocks from the Paleoproterozoic (~2.1 Ga) Wa-Lawra Belt, southeastern margin of the West African Craton, Geodinamica Acta, 31:1, 27-39, DOI: 10.1080/09853111.2019.1670414

To link to this article: https://doi.org/10.1080/09853111.2019.1670414

Published online: 27 Sep 2019.

GEODINAMICA ACTA
2019, VOL. 31, NO. 1, 27–39
https://doi.org/10.1080/09853111.2019.1670414

Taylor & Francis
Taylor & Francis Group

ARTICLE

Geochemical constraints on provenance and source area weathering of metasedimentary rocks from the Paleoproterozoic (~2.1 Ga) Wa-Lawra Belt, southeastern margin of the West African Craton

Daniel K. Asiedu[a], Magdalene Agoe[b], Prince O. Amponsah[a], Prosper M. Nude[a] and Chris Y. Anani[a]

[a]Department of Earth Science, University of Ghana, Accra, Ghana; [b]Technical Department, Azumah Resources Ghana Ltd, Accra, Ghana

ABSTRACT

The Wa-Lawra Belt which is situated in the northern part of Ghana consists of Paleoproterozoic Birimian fine metasedimentary rocks metamorphosed to greenschist facies, particularly, in the western part. A whole-rock geochemical study of these metasedimentary rocks was undertaken to unravel their source area weathering, provenance and tectonic setting. Geochemical characteristics of the studied shales show that they are immature in nature and first cycle in origin, with little or no recycled component. Compared to Post-Archaean Australian Shales (PAAS), the studied shales indicate reduction in Zr, Hf, La, Nb, Th and Ta being the high field strength elements and evidences of transition metal enrichments in V, Ni, Sc, Co, and Cr. Major element geochemistry indicates that the shales were subjected to slight potassium metasomatism after deposition. Pre-metasomatized Chemical Index of Alteration calculations indicates that weak to moderate degree of chemical weathering took place at the sediment source area. Co-Th-La-Sc systematics reveals a combination of mafic and felsic provenances for the shales. Eu/Eu* together with values of Th/U and some abundances of trace elements show that the shales were mainly derived from juvenile rocks. Average REE model calculations suggest that the source materials are composed of about 49% basalt, 16% TTG and 35% granite.

ARTICLE HISTORY
Received 15 April 2019
Accepted 17 September 2019

KEYWORDS
Birimian; geochemistry; metasedimentary rocks; provenance; Wa-Lawra Belt

1. Introduction

The West African craton (WAC) is divided into the Reguibat shield and Leo-man shield to the north and south respectively, comprising Archaean rocks of Liberian age (3.0–2.5 Ga) to the west and the Birimian Paleoproterozoic age to the east of the Leo-Man shield, respectively (Figure 1). The Birimian is made up of four metasedimentary basins and six volcanic belts. The volcanics within the belts comprise low grade metamorphosed lavas that are mainly tholeiitic in composition, 'belt type' tonalite-granodiorite intrusions as well as minor felsic volcaniclastics (Hirdes, Davis, & Eisenlohr, 1992). The basins consist of volcaniclastics, argillites intruded by extensive, late-kinematic 'basin type' granitoid plutons which vary from tonalite to peraluminous granite in composition and wackes which are isoclinally folded (Davis, Hirdes, Schaltegger, & Nunoo, 1994; Hirdes et al., 1992; Leube, Hirdes, Mauer, & Kesse, 1990).

Geochronological as well as geochemical studies of igneous rocks indicate that the main Paleoproterozoic crustal growth events in the WAC are characterised by the formation of huge volumes of juvenile material with the involvement of a significantly small Archaean crust component (Abouchami, Boher, Michard, & Albarede, 1990; Taylor, Moorbath, Leube, & Hirdes, 1992). The processes involved in the growth of the Paleoproterozoic continental crust have always aroused debate amongst various researchers. Workers such as Abouchami et al. (1990) and Boher, Abouchami, Michard, Albarède, and Arndt (1992) have suggested that within the Birimian, a relationship does exist between the tholeiitic magmatism and an oceanic plateau environment whereas several others have proposed that the entire Birimian crust grew in an island arc environment (Ama Salah, Liégeois, & Pouclet, 1996; Beziat et al., 2000; Sylvester & Attoh, 1992). It has further been indicated that the Birimian of the Haute-Comoé was deposited in an intracontinental trans-tensional back-arc basin (Vidal & Alric, 1994). This suggests a pre-Birimian basement existed.

The Birimian Supergroup in Ghana consists of narrow sedimentary basins that trend northeasterly as well as linear greenstone belts consisting mainly of volcanic, volcaniclastic to clastic series. Both the sedimentary basins and the greenstone belts (one of which is the Lawra belt – the study area) are intruded by various generations of granitoids (Figure 2). These volcanic and metasedimentary supracrustal rocks occurred during an accretionary period around 2.1 Ga (Abouchami et al., 1990; Taylor et al., 1992) during the 2.1–2.0 Ga Eburnean orogeny (Bonhomme, 1962). The supracrustal sequence was folded and

CONTACT Chris Y. Anani cyanani@ug.edu.gh Department of Earth Science, University of Ghana, P.O. Box LG 58, Legon, Accra, Ghana

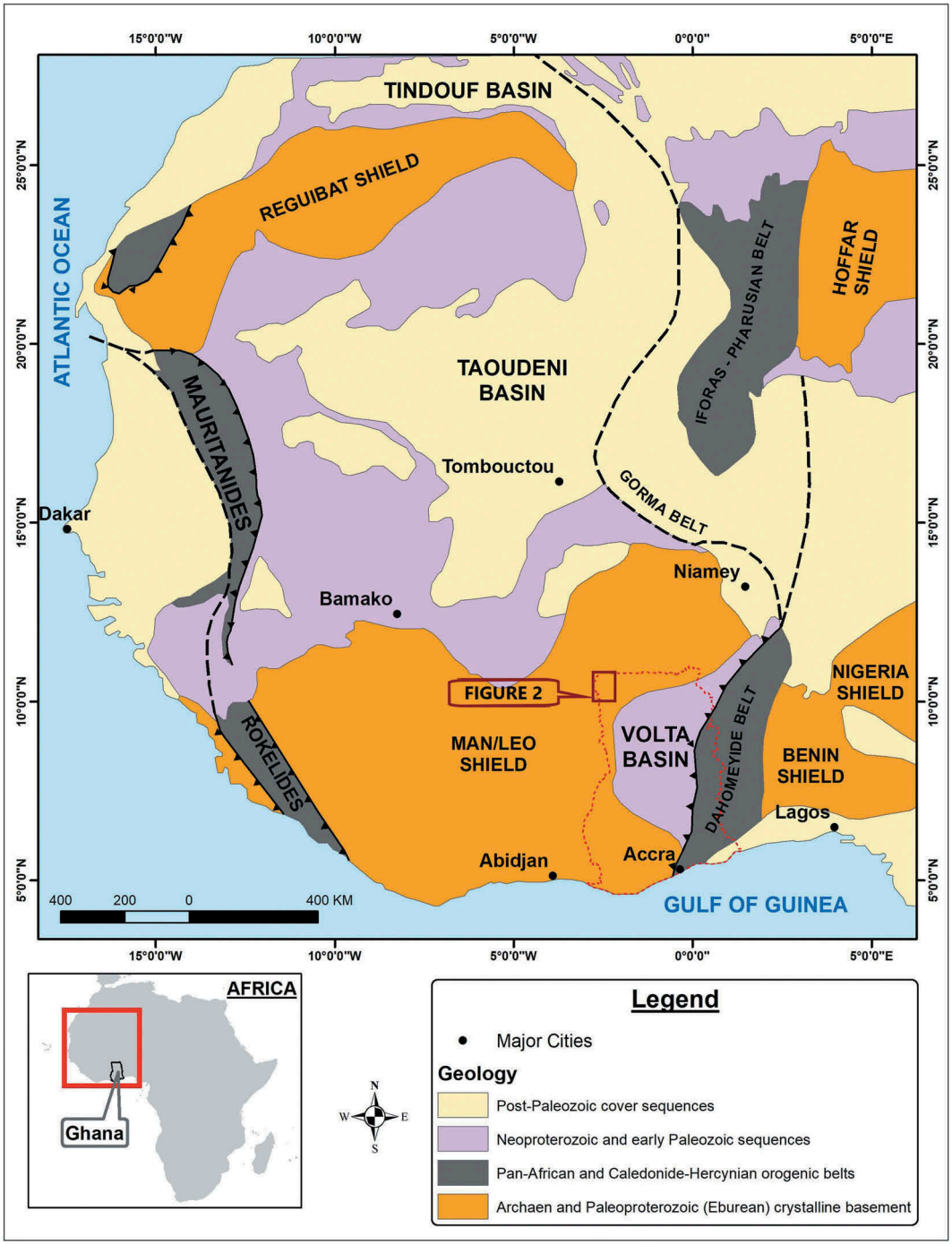

Figure 1. Simplified geological map of the Leo-Man Shield of the West African Craton (WAC) indicating the position of Ghana modified after Carney et al. (2010). Inset showing a simplified map of Africa showing the position of Ghana.

metamorphosed under predominantly greenschist facies conditions. To the east of the Birimian Supergroup is a relatively younger surrounding unit which is the Voltaian Supergroup Figures 1 and 2 (insert). The Voltaian Supergroup fills the Volta Basin (Figure 2, insert) which is made up of Neoproterozoic to early Paleozoic strata up to ~5 km thick. The strata consist of a succession of sandstones, mudstones, and few proportions of limestone (Affaton, Sougy, & Trompette, 1980; Anani, Mahamuda, Kwayisi, & Asiedu, 2017; Kalsbeek, Frei, & Affaton, 2008). It covers a surface area of ~115,000 km^2.

In Ghana, the basement rocks to the Birimian are not known. Extensive geochemical and isotopic studies of igneous rocks (i.e. volcanic rocks and associated granitoids) indicate that the Birimian constitutes a huge addition of materials from the mantle (e.g. Dampare et al., 2009; Sakyi et al., 2018, 2014) although the terrane may be underlain substantially by Archaean basement. In Ghana, the metasedimentary rocks in the Birimian Supergroup have received relatively less attention, even though they form the dominant component of the overall Birimian rocks. The crustal evolution of this segment

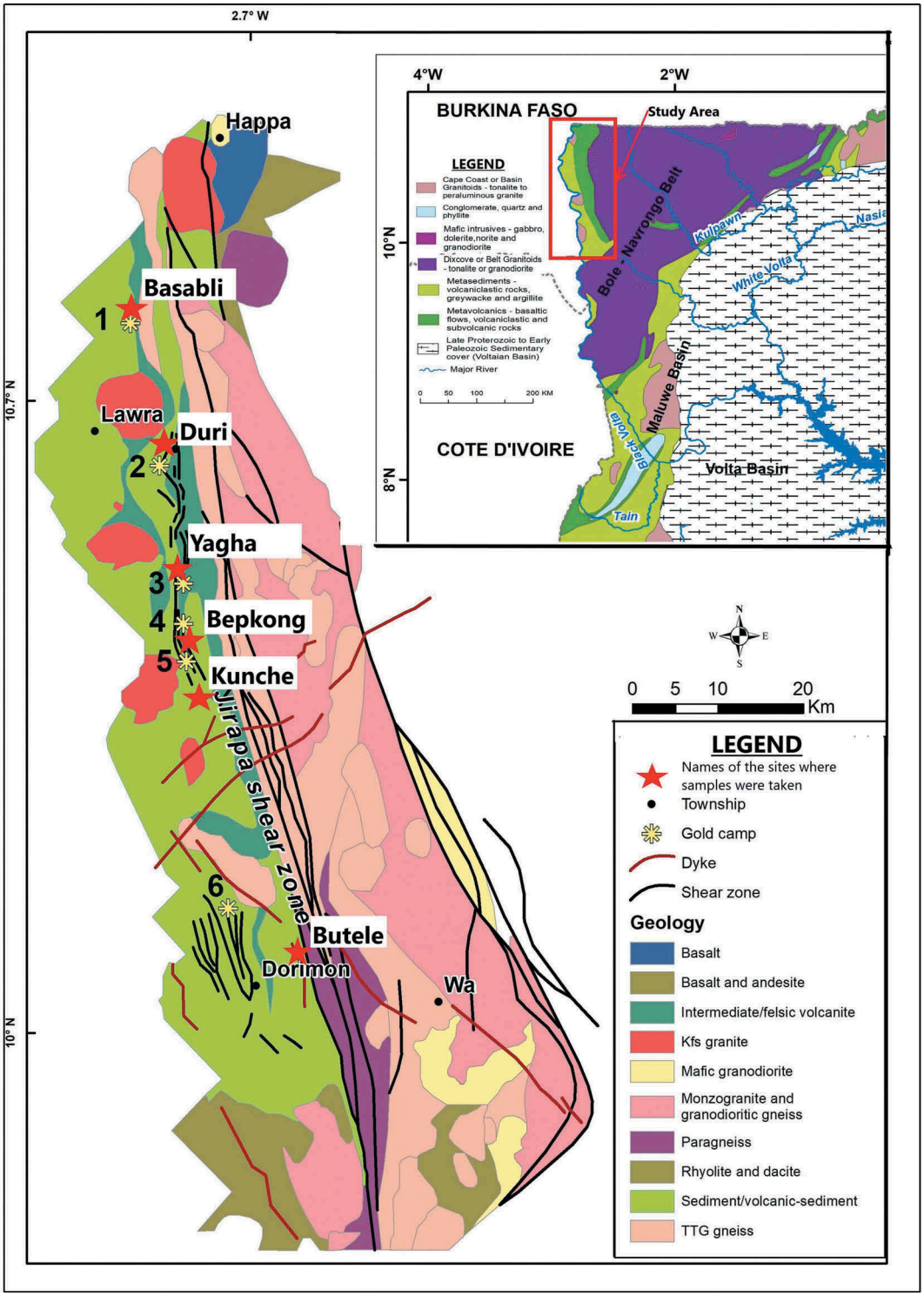

Figure 2. Geological map of the study area modified after Amponsah et al. (2016), showing the various gold camps (where the samples were collected). Insert showing a map of northwestern Ghana showing the surrounding rock units modified after Petersson, Scherstén, and Gerdes (2018).

of the continental crust may be derived by important information from these metasedimentary rocks.

Siliciclastic sedimentary rocks provide an abundance of data about the evolution of the crust. Siliciclastic rock compositions have served as the source of valuable information regarding source-area and tectonic setting (e.g. Bhatia & Crook, 1986), paleoclimate (e.g. Fedo, Eriksson, & Krogstad, 1996; Fedo, Young, & Nesbitt, 1997), as well as average composition estimates of the upper crust (e.g. Condie, 1993; Taylor & McLennan, 1985). This paper presents the outcome of a bulk-rock geochemical study of Birimian metasediments of the Lawra belt, northwestern Ghana; the scanty geochemical studies of the metasedimentary rocks of the Birimian Supergroup in Ghana have been restricted to southwestern Ghana (Asiedu et al., 2017, 2004). This study aims at (i) defining the geochemical features of the

metasedimentary rocks, (ii) discussing conditions that prevailed at the source area regarding paleoweathering, and (iii) constraining their tectonic setting and provenance.

2. Geological setting

The Wa-Lawra greenstone belt in NW Ghana forms a section of the Eastern Paleoproterozoic Birimian terrane within the WAC (Amponsah et al., 2016; Block et al., 2015; Griffis, Barning, Agezo, & Akosah, 2002). This Paleoproterozoic Birimian geology extends into countries such as Burkina Faso, Ivory Coast, Mali, Niger and Ghana. The Wa-Lawra greenstone belt trends N-S (Kesse, 1985; Somakin and Lashmanov, 1991) in Ghana whilst all other belts trends NE-SW. It is the southern extension of the N-S trending Bromo belt which runs from Burkina Faso into Ghana (Amponsah et al., 2016; Baratoux et al., 2011). The Wa-Lawra belt in Ghana is bounded by the Diebougou-Bouna granitoid domain to the west in Ivory Coast. It is fault bounded (i.e. Jang Fault which is a NNW-S splay of the main Jirapa fault) by the 2162 ± 1Ma to 2134 ± 1Ma Koudougou-Tumu granitoid terrane composed of gabbro and gneisses. These have porphyritic granite intrusions of 2128 Ma to the east (Block et al., 2015). In the south, it is bounded by the Bole-Nagondi belt and the Bole-Bulenga domain. According to Block et al. (2015) and Amponsah et al. (2015, 2016), the Wa-Lawra belt is divided into two halves, with each half juxtaposed by the crustal-scale transcurrent sinistral Jirapa fault. Jirapa faults crosscuts the Bole-Bolenga domain and integrates with the Bole-Nagondi belt in the south (Block et al., 2015; DeKock et al., 2012). The western portion consists mainly of basalts (2200–2160 Ma; Baratoux et al., 2011), (2139 ± 2 Ma detrital zircon ages; Agyei Duodu et al., 2009), sediments (intercalated suites of meta-shales, meta-siltstone and meta-arenites), volcaniclastic rocks and intrusive granitoids of varying ages (i.e. 2212 ± 1 Ma; Sakyi et al., 2014). All the rocks in this half have experienced greenschist metamorphism. P-T conditions obtained from mica schist in the eastern half from a chlorite-quartz-water (Chl-Qz-H_2O) and phengite-quartz-water (Ph-Qz-H_2O) equilibria defined a P-T space of 310-380°C at 2 kbar (Block et al., 2015). Based on micro-thermometric analysis done, CH_4-H_2O ± SO_2 and H_2O-CH_4 -CO_2-SO_2 fluid inclusions by Amponsah et al. (2016) indicated that greenschist facies hydrothermal fluids circulated in the rock at temperatures 310 to 370°C. The eastern half of the Wa-Lawra belt is composed of amphibolite, para and ortho-gneisses, granitoids and rhyolites (Amponsah et al., 2016; Block et al., 2015). The amphibolite facies metamorphism in the eastern half is defined by the mineral assemblage hornblende, clinopyroxene and plagioclase (Block et al., 2015).

A multiphase deformational episode has been recognised on the Wa-Lawra belt by several workers (Amponsah et al., 2016; Baratoux et al., 2011; Block et al., 2015). The first deformation event on the belt is recognised as a result of a sinistral anastomosing transcurrent shear zone showing steep dips. It is oriented N to NNW (left lateral sinistral jog) or fault (along the Jirapa and Jang fault) and denotes an ESE-WNW and E-W shortening (Amponsah et al., 2016). This structural grain resulted from a long-protracted deformation episode from 2128Ma to 2086Ma. This affected all the volcaniclastic sediments, sedimentary and volcanic rocks within the belt (Baratoux et al., 2011). A N-NNW striking and vertically dipping penetrative foliation (S1) is evidence of this structural grain. Further evidence is a sub-horizontal stretching lineation which trends northwards and plunges 20° and parallel to the S0 bedding planes. The second deformational episode is marked by E-W tension gashes. They crosscut S1 shear zones and are mostly quartz filled with E-W direct shortening. The 2020 Ma to 2000 Ma last deformational episode in the belt is marked by F3 isoclinal fold and crenulation cleavages. Vertical fold axes mark the F3 folds as well as axial planar S3 foliation which is ENE-WSW. This deformational episode is assumed to indicate N-S shortening.

3. Sampling and analytical methods

Forty-one (41) samples were collected from thirty (30) drill holes from the following areas in the western part of the Wa-Lawra belt: Basabli, Duri, Yagha, Benkpong, Kunche and Butele (Figure 2). Twenty-two (22) shale samples devoid of weathering and alterations were selected. These were subjected to whole-rock geochemical analysis. The whole-rock major and trace element (including REE) analysis was performed by ALS laboratory in Vancouver, Canada. Sample preparation was done by placing sample (1.0 g) in an oven at 1000°C for 1 hour, cooled and then weighed. The percent loss on ignition was calculated from the difference in weight.

The major elements were analysed by Inductively Coupled Plasma-Atomic Emission Spectroscopy (ICP-AES). This was first achieved by dissolution of the grounded samples by lithium metaborate/lithium tetraborate ($LiBO_2$/$Li_2B_4O_7$) fusion method. This involved mixing lithium metaborate/lithium tetraborate flux with a prepared sample (0.200 g) and fused in a furnace at 1025°C. An acid mixture containing nitric, hydrochloric and hydrofluoric acids was then used to cool and dissolve the mixture. The solution was then analysed by ICP-AES. The results were corrected for spectral inter-element interferences. 0.01% was the

detection limit for the major element oxides (SiO_2, Na_2O, Fe_2O_3, Al_2O_3, MnO, TiO_2, CaO, P_2O_5, K_2O and MgO).

The trace element analyses were performed observing the protocols as for the major element analyses. However, the prepared sample weighed 0.100 g and the analysis was done by Inductively Coupled Plasma – Mass Spectroscopy (ICP-MS). The base metals were analysed using the ICP-AES by sample (about 0.25 g) digestion with perchloric, nitric, hydrochloric and hydrofluoric acids and addition of dilute hydrochloric acid. The detection limits (ppm) for the trace elements are as follows: 1 (Co, Cu, Mo, Ni, Sc, Sn, W), 5 (As, V), 2 (Pb, Zn, Zr) 10 (Li, Tl, Cr,), 0.05 (Th, U, Dy, Cd), 0.1 (Sr, Ta, Ca, Nd), 0.2 (Rb, Hf, Nb), 0.5 (Ag, Cd, Y, Ba, Ce, La), 0.03 (Pr, Sm, Yb, Er, Eu), 0.01 (Tm, Tb, Cs, Ho).

4. Results

The results of the geochemical analysis and their corresponding sample locations are shown in Tables 1 and 2 respectively.

4.1. Major elements

The studied metasedimentary rocks generally have SiO_2 (53.9 to 68.6) wt.%, Al_2O_3 (14.5 to 20.5) wt.%, TiO_2 (0.55 to 1.0) wt.% and P_2O_5 (0.11 to 0.21) wt.% contents similar to that of PAAS (Figure 3). However, Fe_2O_3 (6.39 to 10.15) wt.%, MgO (2.2 to 4.5) wt.% and Na_2O (0.94 to 3.63) wt.% contents are enriched whereas CaO (0.24 to 2.21) wt.% and K_2O (1.17 to 3.70) wt.% contents are generally depleted compared to that of PAAS (Figure 3). They have low SiO_2/Al_2O_3 values (2.73 to 4.73) indicative of their low maturity. SiO_2 correlates negatively with Al_2O_3 ($r = -0.88$), TiO_2 ($r = -0.81$), MgO ($r = -0.88$), and Fe_2O_3 ($r = -0.81$) (Figure 4). P_2O_5, K_2O, MnO and CaO do not systematically vary with SiO_2. However, Na_2O ($r = 0.19$) shows weak positive correlation with SiO_2 (Figure 4).

Several workers have used major element whole-rock geochemisty to classify siliciclastic sedimentary rocks (e.g. Blatt, Middleton, & Murray, 1980; Crook, 1974; Herron, 1988; Pettijohn, Potter, & Siever, 1972). By their Fe_2O_3/K_2O versus SiO_2/Al_2O_3 the studied samples classify as both Fe-shales and shales (Figure 5). The Fe-shales have comparable SiO_2, moderately lower Al_2O_3 and higher Fe_2O_3 contents than the shales.

4.2. Trace elements

The concentrations of the large ion lithosphere elements (LILE) Cs, Rb, Ba and Sr range from 2.59 to 12.1 ppm, 45.8 to 110 ppm, 218 to 879 ppm, and 110 to 394 ppm, respectively (Table 1). In comparison to PAAS, the studied shales exhibit slight to strong depletion in Rb, Ba and Cs and enrichment in Sr. Rb/Sr ratios (0.2 to 0.93) are lower than that of PAAS (Rb/Sr = 1.25; Taylor & McLennan, 1985).

The studied shales have high so-called transition metals Ni (73 to 120 ppm, average of 94.5 ppm), Co (21 to 35, average of 27.4 ppm), Cr (150 to 260 ppm, with an average of 190 ppm), V (110 to 180 ppm, with average of 151 ppm), and Sc (16 to 24 ppm, with an average of 19.8 ppm). Generally, the studied shales are enriched in these transition metals relative to PAAS (Figure 6).

The concentrations of the high field strength elements (HFSE), Zr, Hf, Ta, Nb, Th, U, Y, La range from 103 to 163 ppm, 2.8 to 4.1 ppm, 0.2 to 0.4 ppm, 4.6 to 7.1 ppm, 2.26 to 3.86 ppm, 0.9 to 1.45 ppm, 9.2 to 22.2 ppm, 11.8 to 23 ppm, respectively. Relative to PAAS the studied shales exhibit depletion in the HFSE (Figure 6). The average Zr/Hf value of 36.6 is suggestive of zircon control ($Zr \approx 40$). Th/U values (2.33 to 3.14) are consistently lower than that of the continental upper crust ($Th/U \approx 3.8$; McLennan, Hemming, McDaniel, & Hanson, 1993).

4.3. Rare earth elements

The rare earth element (REE) data for the studied shales are somewhat variable with total REE (ΣREE) values of 65.7 to 127 ppm, averaging of 101 ppm, which is lower than that of PAAS value of 184.8 ppm (Taylor & McLennan, 1985). The shales display REE patterns that are similar when normalised to PAAS with slightly depleted Light REE (LREE) (Figure7), positive Eu-anomaly and fairly flat Heavy REE (HREE). On a chondrite-normalised diagram (not shown) the studied shales display fractionated LREE patterns (average $La_N/Sm_N = 2.81$), small negative Eu (average $Eu/Eu^* = 0.79$) and fairly flat HREE patterns (average $Gd_N/Yb_N = 1.51$) which are characteristic of sediments derived from upper continental crust (Taylor & McLennan, 1985).

5. Discussion

5.1. Heavy mineral accumulation and metamorphism

The degree of sorting and recycling may be deduced by evaluating the accumulation of weathering-resistant phases such as zircon and monazite in siliciclastic sedimentary rocks (McLennan et al., 1993). Enrichment of zircon, and therefore recycling and sorting, can be inferred from the Th/Sc versus Zr/Sc diagram; the ratio Zr/Sc is an effective index of zircon enrichment while the ratio Th/Sc is a good indicator of igneous chemical differentiation processes (McLennan et al., 1993). The studied samples on this diagram trend in the general provenance-dependent compositional variation pattern with none of the

Table 1. Geochemical data for the metasedimentary rocks of the Wa-Lawra belt.

SAMPLE	BR223	BR258	BR302	BR203	BR263	BR450a	BR450b	BR265	KR699	KR695	KR700a
SiO_2	59.6	58.1	61.9	57.7	61.4	64.3	55.6	62.1	56.1	60.6	64.2
Al_2O_3	17.0	16.2	16.0	18.2	15.2	14.7	18.7	16.1	19.6	17.7	16.6
Fe_2O_3	9.08	8.81	8.59	9.08	7.18	7.53	9.79	7.91	8.44	6.70	6.39
CaO	1.11	1.92	0.63	0.62	2.07	0.97	0.99	1.03	2.21	2.07	0.85
MgO	3.68	3.80	3.43	3.70	3.31	2.98	3.87	3.17	3.47	3.21	2.89
Na_2O	3.22	2.12	3.45	3.20	3.52	3.29	3.56	3.48	3.05	3.11	3.63
K_2O	1.53	2.18	1.33	1.97	1.59	1.17	1.76	1.48	2.95	2.39	2.24
TiO_2	0.66	0.66	0.65	0.76	0.59	0.62	0.73	0.71	0.80	0.61	0.64
MnO	0.11	0.09	0.09	0.06	0.09	0.08	0.10	0.06	0.07	0.07	0.06
P_2O_5	0.11	0.16	0.11	0.12	0.14	0.12	0.19	0.17	0.17	0.11	0.14
LOI	4.51	5.33	4.19	4.35	5.49	3.68	4.66	3.80	3.78	2.94	2.82
Total	100.56	99.32	100.32	99.71	100.53	99.44	99.95	100.01	100.64	99.46	100.41
Rb	58.9	83.2	53.6	72.9	59.6	45.8	71.3	53.1	87.7	80.3	76.0
Sr	282	233	182	241	297	154	178	261	394	355	141
Ba	246	422	222	373	376	218	324	395	720	653	714
Th	2.96	2.97	2.95	2.97	2.76	2.26	3.49	2.91	3.43	2.98	2.77
U	0.99	1.10	0.94	1.06	1.08	0.91	1.27	1.06	1.23	1.11	1.18
Zr	113	112	110	122	111	103	129	118	130	127	131
Hf	3.4	3.2	3.2	3.5	3.3	2.9	3.7	3.3	3.9	3.3	3.5
Nb	5.2	5.2	5.0	5.7	4.7	4.6	5.6	5.4	6.0	4.8	4.9
Ta	0.3	0.3	0.3	0.3	0.3	0.2	0.3	0.3	0.3	0.3	0.3
Y	17.4	17.2	16.6	19.9	15.6	14.4	20.9	15.6	19.3	9.2	14.6
Sc	22	20	22	21	17	17	21	18	23	16	16
V	169	151	151	175	131	128	156	136	176	137	140
Cr	170	170	150	190	190	180	180	190	200	210	230
Co	30	26	29	31	24	26	32	25	29	22	24
Ni	100	110	94	102	83	85	105	90	101	73	80
La	13.4	18.0	16.8	16.2	17.1	11.8	21.4	17.4	21.1	18.2	16.0
Ce	29.1	38.2	35.6	36.1	35.4	25.5	45.0	36.3	44.4	37.6	35.4
Pr	3.52	4.78	4.42	4.46	4.43	3.14	5.53	4.58	5.39	4.63	4.32
Nd	14.0	19.4	17.7	18.5	17.7	12.7	22.8	18.3	22.2	18.4	17.2
Sm	2.94	3.98	3.50	4.04	3.58	2.57	4.50	3.54	4.34	3.41	3.40
Eu	0.90	1.02	0.82	0.93	0.94	0.68	1.15	0.85	1.25	0.88	0.80
Gd	2.68	3.39	3.33	3.48	3.03	2.41	3.78	3.05	3.65	2.55	2.84
Tb	0.46	0.51	0.46	0.52	0.48	0.39	0.65	0.48	0.57	0.29	0.47
Dy	2.74	3.10	2.83	3.52	2.79	2.41	3.69	2.80	3.51	1.55	2.58
Ho	0.61	0.64	0.61	0.74	0.59	0.54	0.75	0.58	0.70	0.33	0.53
Er	1.95	1.87	1.70	2.18	1.67	1.57	2.10	1.56	2.07	1.10	1.52
Tm	0.28	0.28	0.26	0.30	0.26	0.23	0.29	0.21	0.30	0.21	0.24
Yb	1.91	1.89	1.79	2.03	1.63	1.55	1.97	1.58	2.11	1.26	1.61
Lu	0.32	0.29	0.27	0.32	0.26	0.23	0.33	0.26	0.32	0.22	0.24

SAMPLE	KR7002a	KR080a	KR0802b	KR700b	KR7002b	KR565	AVA042a	AVA042b	AVA043	AVA038a	AVA038b
SiO_2	57.7	58.9	57.7	58.1	56.2	58.1	63.8	68.6	59.3	53.9	59.9
Al_2O_3	18.2	18.3	18.5	18.3	18.4	17.8	15.7	14.5	17.8	20.5	17.9
Fe_2O_3	9.67	8.61	9.51	8.87	9.40	8.43	7.90	6.93	8.40	10.2	8.40
CaO	1.86	1.28	1.16	1.02	1.22	1.25	0.30	0.24	0.41	0.60	1.16
MgO	4.50	3.99	4.01	4.17	4.41	3.98	3.01	2.43	3.55	4.47	3.59
Na_2O	2.63	2.16	1.91	1.64	1.44	1.73	3.09	0.94	3.31	1.18	2.17
K_2O	2.02	2.84	3.02	3.18	3.18	3.01	1.49	2.34	1.66	3.10	2.01
TiO_2	0.72	0.73	0.73	0.72	0.69	0.70	0.59	0.55	0.68	0.81	0.77
MnO	0.10	0.09	0.09	0.09	0.09	0.09	0.10	0.05	0.10	0.07	0.07
P_2O_5	0.20	0.18	0.19	0.16	0.18	0.16	0.16	0.13	0.21	0.19	0.16
LOI	4.34	4.13	4.09	4.59	4.92	4.70	3.85	3.76	4.40	5.25	4.55
Total	101.89	101.21	100.86	100.79	100.08	99.9	99.94	100.47	99.77	100.22	100.68
Rb	73.0	99.5	108	108	103	102	54.0	83.2	60.6	110	74.5
Sr	289	207	154	125	110	139	195	144	145	165	308
Ba	543	463	498	872	879	830	551	729	427	720	545
Th	3.2	3.43	3.34	3.55	3.40	3.38	3.07	2.74	2.98	3.86	3.32
U	1.34	1.30	1.29	1.27	1.24	1.45	1.00	0.90	1.18	1.28	1.17
Zr	135	137	137	139	129	134	132	107	163	156	134
Hf	3.5	3.4	3.7	3.9	3.6	3.6	3.4	2.8	4.0	4.1	3.6
Nb	5.8	5.8	5.7	5.9	5.6	7.1	6.3	4.8	5.3	6.2	6.1
Ta	0.4	0.4	0.4	0.4	0.4	0.4	0.3	0.3	0.3	0.4	0.4
Y	20.1	19.8	20.1	17.7	19.9	17.8	17.3	15.0	18.5	22.2	17.1
Sc	21	21	21	20	21	21	16	18	19	24	20
V	163	163	155	160	159	161	110	126	150	180	146
Cr	180	200	210	180	160	180	160	160	260	220	210
Co	28	30	30	27	27	29	22	21	27	35	29
Ni	101	99	100	94	98	94	80	81	87	120	102
La	21.6	21.3	21.9	18.1	22.7	17.3	22.0	15.1	18.4	23.0	20.7
Ce	47.3	46.7	48.4	39.4	48.4	38.6	46.3	32.5	40.6	49.9	45.2
Pr	5.74	5.85	5.86	4.91	6.02	4.85	5.61	4.01	4.95	6.18	5.57
Nd	24.2	23.0	24.8	20.6	24.1	20.6	22.8	16.1	21.0	26.0	23.0
Sm	4.79	5.00	5.19	4.47	5.42	4.24	4.71	3.61	4.33	5.28	4.68
Eu	0.95	1.18	1.17	0.89	1.01	0.98	1.15	0.87	1.09	0.99	0.96
Gd	3.86	4.44	4.15	3.68	4.34	3.71	3.65	2.80	3.54	4.52	3.60
Tb	0.59	0.63	0.64	0.53	0.66	0.53	0.52	0.42	0.55	0.73	0.54

(*Continued*)

Table 1. (Continued).

SAMPLE	BR223	BR258	BR302	BR203	BR263	BR450a	BR450b	BR265	KR699	KR695	KR700a
Dy	3.35	3.50	3.56	3.14	3.68	3.20	3.06	2.61	3.25	3.87	2.92
Ho	0.73	0.72	0.78	0.66	0.75	0.66	0.69	0.58	0.70	0.89	0.64
Er	2.18	2.20	2.29	2.03	2.06	1.99	1.75	1.65	1.99	2.42	1.85
Tm	0.33	0.32	0.33	0.31	0.34	0.29	0.30	0.23	0.29	0.39	0.30
Yb	1.93	2.05	2.05	2.10	2.12	2.01	1.80	1.47	2.01	2.35	1.82
Lu	0.34	0.33	0.34	0.31	0.34	0.33	0.28	0.26	0.32	0.37	0.29

Major elements in wt.%, trace elements in ppm.

Table 2. Sample locations of the metasedimentary rocks (Table 1) of the Wa-Lawra Belt.

Sample 1D/Depth	Easting	Northing	Rock name	Sample type
AVA038a (211.0–211.5 m)	524,468	1,166,276	SHALE	CORE
AVA038b (217.5–218.0 m)	524,468	1,166,276	SHALE	CORE
AVA042a (194.0–194.5 m)	524,420	1,166,079	SHALE	CORE
AVA042b (201.1–201.6 m)	524,420	1,166,079	SHALE	CORE
AVA043 (202.0–202.5 m)	524,765	1,166,074	SHALE	CORE
BR203 (251.5–252.0 m)	527,047	1,152,225	SHALE	CORE
BR223 (84.4–85.0 m)	527,186	1,151,474	SHALE	CORE
BR258 (117.5–118.0 m)	527,046	1,152,173	SHALE	CORE
BR263 (144.5–145.0 m)	527,076	1,152,123	SHALE	CORE
BR265 (147.7–218.2 m)	527,050	1,152,095	SHALE	CORE
BR302 (185.5–186.0 m)	527,022	1,152,224	SHALE	CORE
BR450a (228.0–228.5 m)	527,052	1,152,351	SHALE	CORE
BR450b (234.0–234.5 m)	527,052	1,152,351	SHALE	CORE
KR080a (150.0–151.0 m)	527,028	1,149,108	SHALE	CORE
KR0802b (156.0–156.5 m)	527,028	1,149,108	SHALE	CORE
KR565 (163.0–163.5 m)	526,845	1,149,499	SHALE	CORE
KR695 (229.5–230.0 m)	526,990	1,148,778	SHALE	CORE
KR699 (276.0–276.5 m)	526,992	1,148,575	SHALE	CORE
KR700a (229.0–229.5 m)	524,765	1,166,074	SHALE	CORE
KR7002a (261.0–261.5 m)	526,925	1,149,247	SHALE	CORE
KR700b (264.0–264.5 m)	526,925	1,149,247	SHALE	CORE
KR7002b (299.0–299.5 m)	526,925	1,149,247	SHALE	CORE

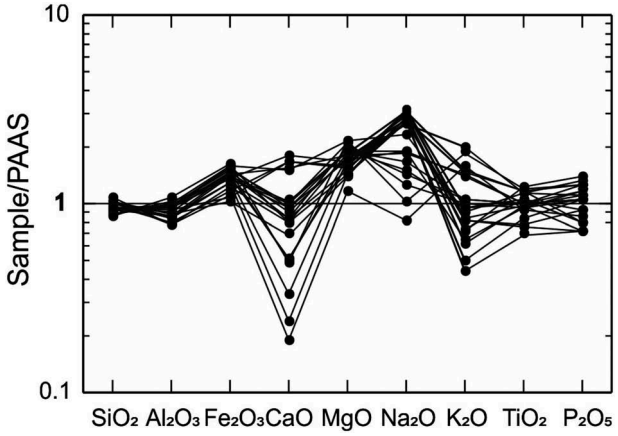

Figure 3. Post-Archaean Australian Shale (PAAS)-normalised major element plots for the studied metasedimentary rocks. PAAS values are from Taylor and McLennan (1985).

samples plotting in the high Zr/Sc range which is characteristic of zircon accumulation associated with sediment sorting and recycling (Figure 8(a)).

Zircon is rich in HREE and its accumulation will result in the decrease in the chondrite-normalised La_N/Yb_N ratio. Therefore, a negative correlation between Zr and La_N/Yb_N would be expected if zircon is concentrated in the samples. However, there is no such negative correlation between the two (Figure 8(b)), and it, therefore, rules out preferential zircon accumulation in the samples. A very steep chondrite-normalised HREE pattern is characteristic of monazite which has very high REE abundances, and even small amounts (<0.01%) result in significant increases in the chondrite-normalised Gd_N/Yb_N ratio (McLennan et al., 1993). The fairly flat HREE pattern of the studied shales (Figure 7) rules out preferential monazite accumulation in the samples.

Some major and trace elements in metamorphic rocks are mobilised by interaction with fluids. To a lesser extent, by solid-state diffusion and melt generation (Rollinson, 1993). The rocks of the Lawra Belt have been subjected to up to greenschist facies metamorphism and therefore there is the possibility that some of the elements may have been preferentially remobilized (Rollinson, 1993; Taylor & McLennan, 1985). Such element remobilization would obviously reduce the effectiveness of using them in provenance discrimination.

To minimise the effect of remobilization, samples containing any visible hydrous fluid transfer veinlets were avoided for this study. Nevertheless, some authentic proofs have been used against large-scale remobilization of the elements in the studied metasedimentary rocks: All the samples have similar and smooth REE patterns which would not be expected during remobilization. In addition, although it is

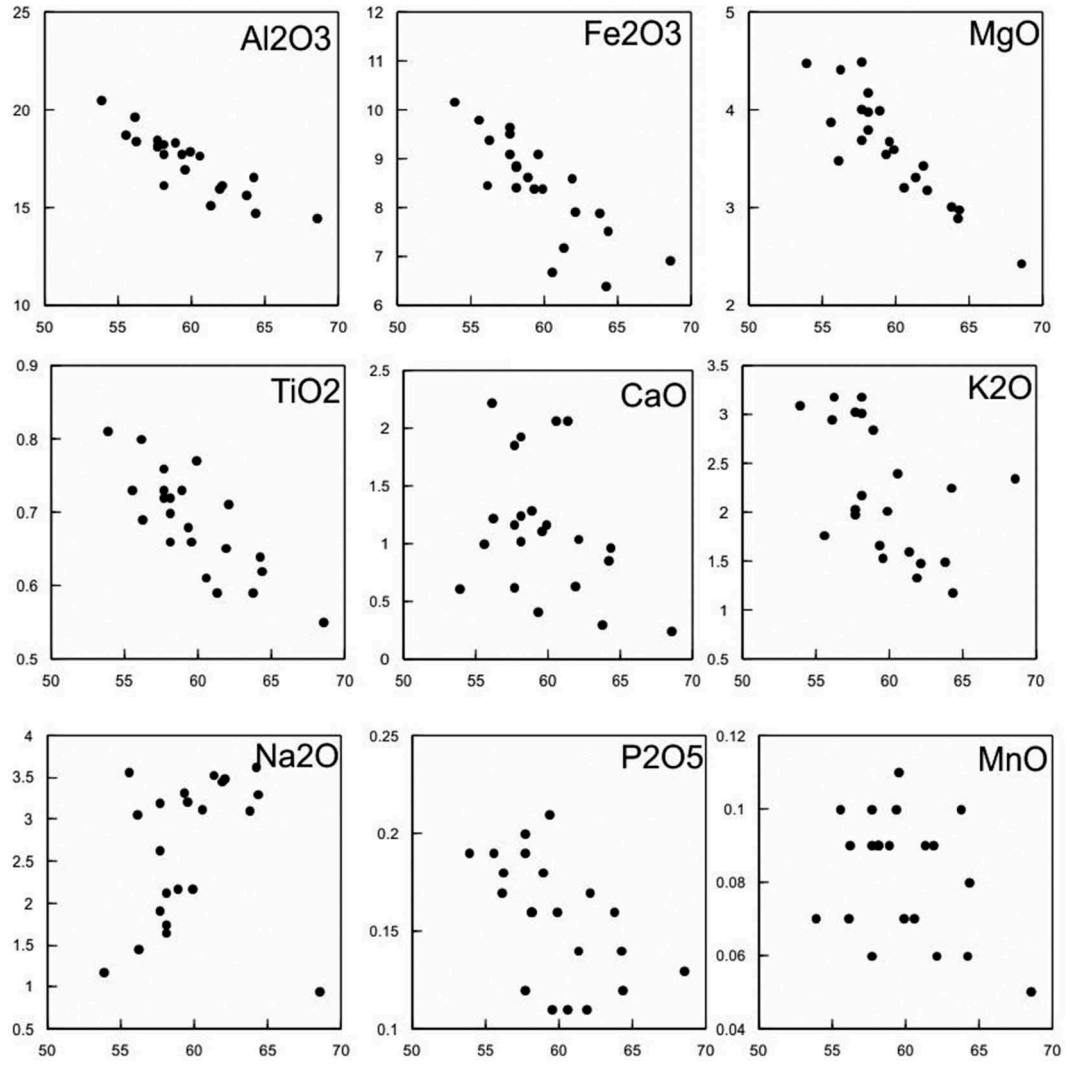

Figure 4. Covariation of major elements versus SiO_2 (wt%) for the studied metasedimentary rocks.

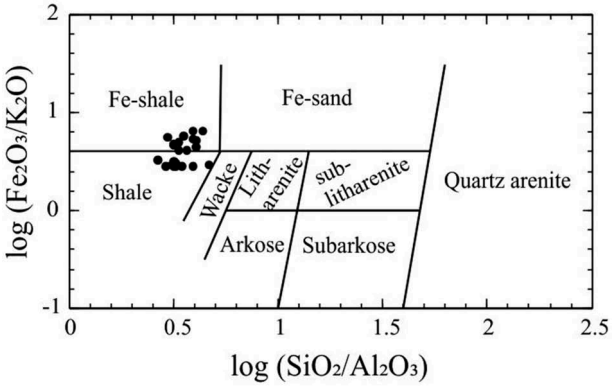

Figure 5. The classification of the studied metasedimentary rocks using log (Fe_2O_3/K_2O) versus log (SiO_2/Al_2O_3) (after Herron, 1988).

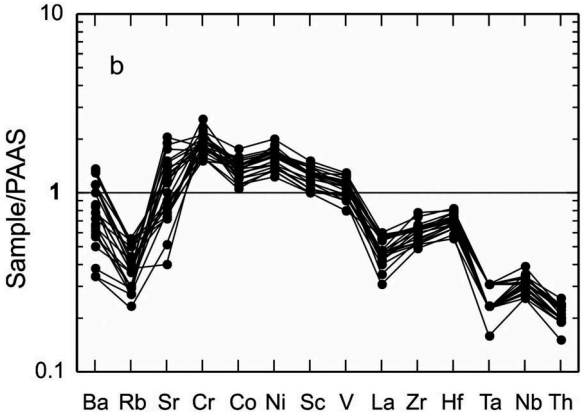

Figure 6. Trace element concentrations of the studied shales normalised to the composition of average PAAS. The normalising values are those of Taylor and McLennan (1985).

possible that some elements such as the LILE may have been remobilized, the covariance among the HFSE such as Zr, Hf, Nb, Ta, Th, U, V, Cr, Ni, Co, and REEs suggests that these elements have the same degree of low mobility during metamorphism.

5.2. Source area weathering and diagenesis

For most rocks, the Rb/Sr ratio increases with increasing degree of chemical weathering. This is so because Rb^+, a large alkali trace element, remains fixed in the

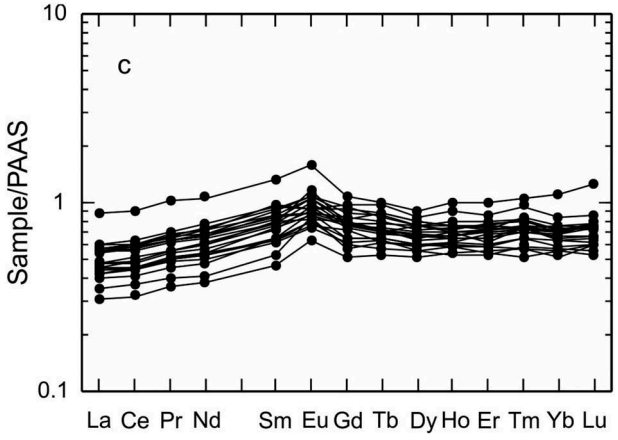

Figure 7. Rare earth element abundances of the studied shales normalised to PAAS. PAAS values are from Taylor and McLennan (1985).

weathered residue, in preference to the smaller Sr^{2+} which is selectively leached (McLennan et al., 1993; Nesbitt et al., 1980). As a result, the Rb/Sr ratio has been used to evaluate the intensity of chemical weathering at the source area; Rb/Sr > 1 is an indication of high degree of chemical weathering whereas Rb/Sr < 1 indicates moderate to low degree of chemical weathering. The studied shales have range of Rb/Sr from 0.20 to 0.93 (average, 0.43) suggesting low degree of chemical weathering at the sediment source area.

For most upper crustal igneous rocks, the Th/U is typically about 3.5 to 4.0 (McLennan et al., 1993). Weathering typically results in the oxidation and subsequent dissolution of U thereby elevating the Th/U ratios above the upper crustal values, especially for shales (Taylor & McLennan, 1985). However, other sedimentary processes may result in U enrichment thereby lowering the Th/U ratio; in such cases the low Th/U will be accompanied by high U content. The Th/U values in the studied shales range from 2.33 to 3.14 (average 2.73) which is well below upper crustal values, and the U concentrations range from 0.9 to 1.45 ppm (average 1.15 ppm) well below that of typical shales (U ~ 3.1) and upper continental crust (U ~ 2.7) (Taylor & McLennan, 1985). This suggests a low degree of chemical weathering at the sediment source area.

The Chemical Index of Alteration (CIA) has been used to quantify the weathering history of sedimentary rocks, primarily to understand paleoclimate conditions (Nesbitt & Young, 1982, 1984). Unweathered igneous rocks have CIA values less than 50, typical shales average about 70 to 75, and intensely weathered rocks have CIA values that approaches 100 (Fedo et al., 1996; McLennan et al., 1993). The studied shales have CIA values that range from 58 to 78 (average, 67.6), which ranges from those of unweathered igneous rocks to typical shales, indicating low to moderate degree of weathering at the sediment source area.

The weathering history for the studied shales may be evaluated using the A-CN-K diagram (Figure 9). In this diagram, it is expected that the samples will plot in a trend parallel to the A-CN join if weathering is the control of the composition (Fedo et al., 1996; Fedo, Nesbitt, & Young, 1995; McLennan et al., 1993). The studied samples, however, indicate a linear trend (Trend 1). It is not comparable with simple weathering being the sole control of the composition (Trend 2). The plots suggest the effects of K addition to the samples as a result of metasomatism (Fedo et al., 1996, 1995). The pre-metasomatized CIA values of the studied samples may be estimated from the diagram using the method outlined by Fedo et al. (1995). This puts the pre-metasomatized CIA range from 60 to 85 (Figure 9) indicating low to moderate degree of chemical weathering in the source area of the sediments.

The occurrence of K enrichment is widespread in Precambrian sedimentary rocks and therefore, Fedo

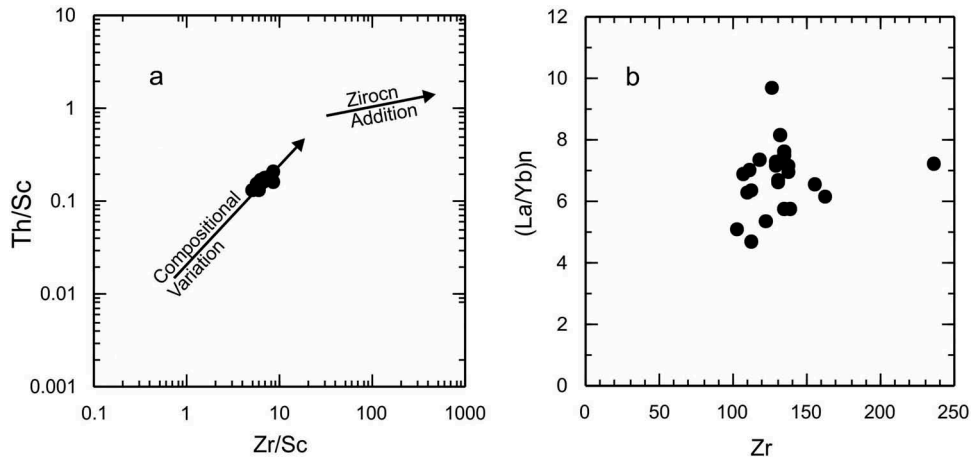

Figure 8. (A) Plot of Th/Sc versus Zr/Sc for the shales of the Wa-Lawra belt. The compositional variation trend lines are from McLennan et al. (1993). (B) Plot of La/Yb versus Zr for the shales of the Wa-Lawra belt.

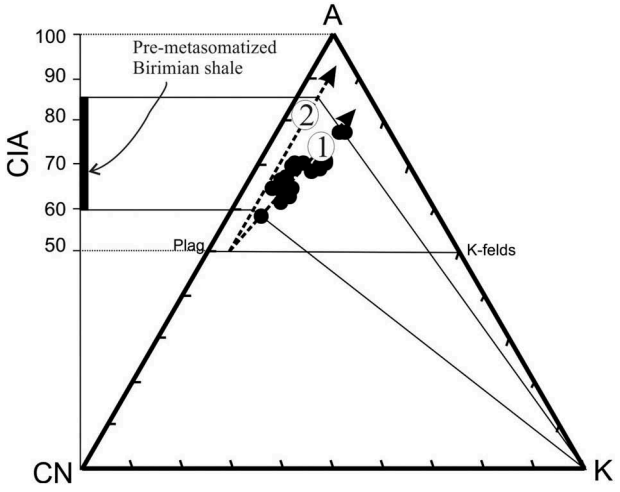

Figure 9. Al_2O_3–(CaO*+Na_2O)–K_2O diagram for the metasedimentary rocks of the Wa-Lawra Belt.

et al. (1996) proposed the Plagioclase Index of Alteration (PIA) to evaluate weathering histories it takes care of the influence of K-feldspar. The maximum PIA value is 100 and unweathered plagioclase has a PIA value of 50. The studied shales have a range of PIA values from 59 to 88 (average, 72) suggesting weak to moderate weathering in the source area of the sediments.

5.3. Source rock composition

The compositions of fine-grained siliciclastic sedimentary rocks, such as shales, are particularly characteristic of the bulk composition of the source region. The abundances of HFSE and the transition metals, and REEs have particularly proved useful in discriminating the source composition of fine-grained metasedimentary rocks (e.g. Asiedu et al., 2017; Roddaz, Debat, & Nikiéma, 2007; Yang, Kyser, & Ansdell, 1998). Compared to PAAS the studied shales show depletion in HFSE such as La, Zr, Hf, Th, Ta, and Nb, and enrichment in transition metals such as Cr, Ni, Co, Sc, and V, suggesting a significant contribution from mafic sources (Figure 6). Compared to PAAS the studied shales show less LREE enrichments and less pronounced europium anomalies (Figure 7) also suggesting significant input from mafic sources.

Co-Th-Sc-La systematics can reveal the mixing between felsic and mafic sources for sedimentary rocks (Taylor & McLennan, 1985; Yang et al., 1998). On La/Sc versus Co/Th and Sc/Th versus Co/Th diagrams (Figure 10(a and b)), the studied Birimian shales plot between the basalt and granite end-members with cluster towards the mafic end (high La/Sc and Co/Th, and low La/Sc). The geochemistry of the studied shales can, therefore, be explained as having been derived from a mixture of basaltic rocks (mainly) and granitic rocks (subordinately).

Following the establishment of diverse possible source components, we seek to indicate the relative contribution of three rock types with distinct REE patterns. These are basalt (BAS), granite (GRA) and tonalite–trondhjemite–granodiorite (TTG). Kasanzu, Makenya, and Manya (2008) were adopted to achieve the mixing calculations. Modelling for the average studied Birimian shale accomplished using the following REE parameters: Gd_N/Yb_N, Eu/Eu*, and La_N/Yb_N. The REE data of the endmembers (i.e. BAS, GRA, and TTG) were extracted from Condie (1993). The mixing calculations were set in a matrix form as:

$$\begin{bmatrix} Eu^* / Eu \\ La_N / Yb_N \\ La_N / Sm_N \end{bmatrix} = \begin{bmatrix} 0.93 & 0.36 & 0.99 \\ 11.62 & 9.19 & 2.73 \\ 3.61 & 3.44 & 1.81 \end{bmatrix} \begin{bmatrix} x \\ y \\ z \end{bmatrix} = \begin{bmatrix} 0.80 \\ 6.76 \\ 2.81 \end{bmatrix}$$

where x = TTG, y = granite (GRA) and z = basalt (BAS). The ratios La_N/Yb_N and Gd_N/Yb_N are chondrite-normalised (Normalising values from Taylor & McLennan, 1985).

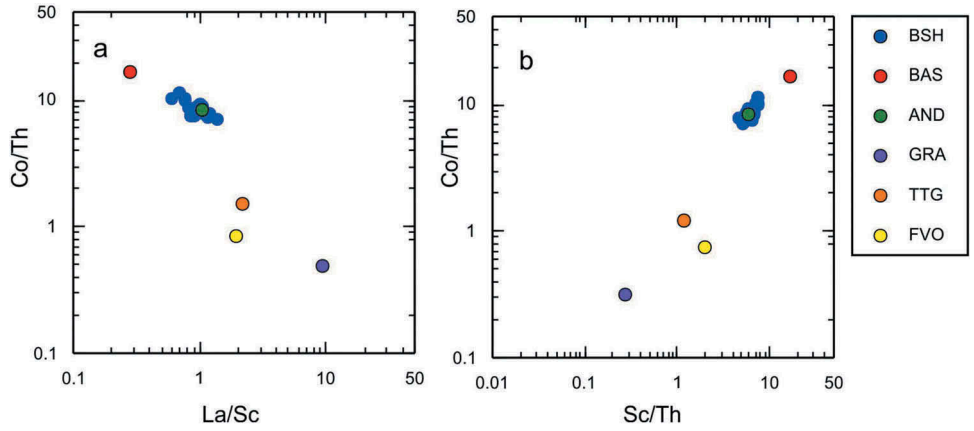

Figure 10. Plots of (A) Co/Th versus La/Sc and (B) Co/Th versus Sc/Th for the metasedimentary rocks of the Wa-Lawra Belt. Also plotted are average Paleoproterozoic volcanic and plutonic rocks from Condie (1993). BSH, studied shales; BAS, basalt; AND, Andesite; GRA, granite; TTG, tonalite–trondhjemite–granodiorite; FVO, felsic volcanic rock.

The results obtained from the mixing calculations have shown that a mixture having 16% TTG, 35% granite and 49% basalt is best for the modelling of the studied Birimian shale.

5.4. Tectonic settings and location of sources

The geochemical compositions of siliciclastic sedimentary rocks have been used to discriminate the tectonic settings of sedimentary basins (e.g. Bhatia, 1983; Roser & Korsch, 1986). Particularly useful for Precambrian metasedimentary rocks are tectonic discrimination diagrams that utilise immobile trace elements (e.g. Bhatia & Crook, 1986). On the Th–Sc–Zr and the Th–La–Sc diagrams, the samples of the Birimian shales fall exclusively in the oceanic island arc field (Figure 11(a and b)).

McLennan et al. (1993) defined four different types of terrane that can be identified from geochemical data: Young Differentiated Arc, Old Upper Continental Crust, Young Undifferentiated Arc, and Recycled Sedimentary Rocks. Compared to PAAS and upper crustal values the studied shales have (i) relatively low but variable SiO_2/Al_2O_3, K_2O/Na_2O, and CIA values, (ii) lower ratios of incompatible to compatible elements, such as Th/Sc and Zr/Sc (Figure 3), and (iii) lack of substantial Eu anomalies and low LREE enrichment (Figure 7). These geochemical features indicate young undifferentiated arc provenance for the studied shales (McLennan et al., 1993). The Th/U ratio is typically about 3.5 to 4.0 for most upper crustal rocks (McLennan et al., 1993; Taylor & McLennan, 1985). Sediments from active margin tectonic settings, which consist of young undifferentiated crust, typically have Th/U significantly below 3.5 accompanied by low Th and U abundances (McLennan and Taylor, 1991; McLennan et al., 1993). On Th/U versus Th diagram (Figure 12), the studied shales mainly plot in the depleted mantle sources field reflecting geochemically depleted mantle sources of the arc provenance. The low Th/U values of the studied shales (Th/U = 2.33 to 3.14) and the relatively low Th and U concentrations compared to upper crustal values and PAAS also suggest that the shales have young undifferentiated arc provenance (Figure 12; McLennan et al., 1993). The above geochemical characteristics, therefore, suggest that the studied Birimian shales are juvenile crustal material derived from local sources, most probably the adjacent volcanic rocks and their associated granitoids.

Our inference that the Birimian shales of the Lawra greenstone belt represent juvenile crustal materials derived locally from the volcanic and associated granitic rocks places constraints on the evolution of the Birimian crust. Our present work, together with previous provenance studies on the Birimian metasedimentary rocks (e.g. Asiedu et al., 2017, 2004) shows juvenile geochemical signatures with only minor contribution of an older crustal component. The lack of evidence for incorporation of substantial Archaean

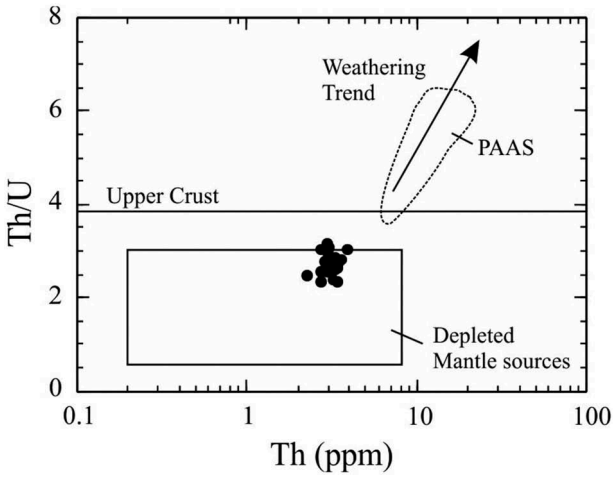

Figure 12. Plot of Th/U versus Th for the shales of the Wa-Lawra belt (after McLennan et al., 1993).

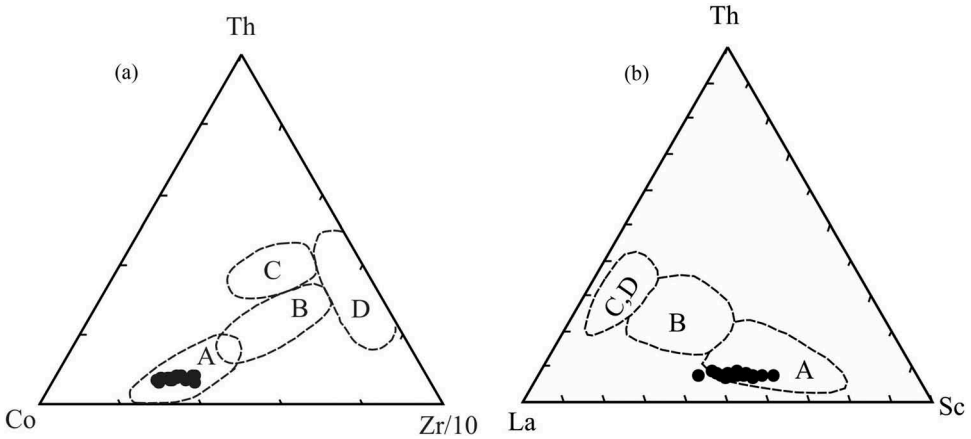

Figure 11. Plots of (A) Th – Co – Zr, and (B) Th – La – Sc for the tectonic setting discrimination of the shales from the Wa-Lawra belt (after Bhatia & Crook, 1986). A, Oceanic Island Arc; B, Continental Island Arc; C, Active Continental Margin; D, Passive Continental Margin.

detritus, therefore, rules out an intra-cratonic origin of the sediments as previously proposed by Ledru, Pons, Milesi, Feybesse, and Johan (1991).

6. Conclusions

A whole-rock geochemical study was undertaken on fine-grained metasedimentary rocks from the Birimian Wa-Lawra Belt of northern Ghana in order to constrain the provenance and source area weathering. The following deductions were made:

(1) The fine-grained metasedimentary rocks are classified as shales on the basis of their major element compositions.
(2) The shales are first cycle in origin and obtained from materials of mixed mafic and felsic compositions. Mixing calculations using the REEs suggest a provenance with mixture having 16% TTG, 35% granite and 49% basalt.
(3) The shales represent juvenile crustal materials derived locally from the associated granitic and volcanic rocks.
(4) The shales were deposited in an oceanic island arc setting.

Acknowledgments

We thank the management and staff of the Exploration Department of the Azumah Resources Ghana Ltd for providing the rock samples for this study, and granting us access to their property for the fieldwork. This research was funded by the Earth Science Capacity Building Project, Department of Earth Science, University of Ghana.

Disclosure statement

No potential conflict of interest was reported by the authors.

ORCID

Chris Y. Anani http://orcid.org/0000-0002-9153-9807

References

Abouchami, W., Boher, M., Michard, A., & Albarede, F. (1990). A major 2.1 Ga event of mantle magmatism in West Africa: An early stage of crustal accretion. *Journal of Geophysical Research*, *95*, 17605–17629.

Affaton, P., Sougy, J., & Trompette, R. (1980). The tectono-stratigraphic relationships between the upper Precambrian and lower Paleozoic Volta Basin and the Pan–African Dahomeyide orogenic belt West Africa. *American Journal of Science*, *280*, 240–248.

Agyei Duodu, J., Loh, G. K., Boamah, K. O., Baba, M., Hirdes, W., Toloczyki, M., & Davis, D. W. (2009). *Geological map of Ghana 1:1 000 000*. Geological Survey Department of Ghana (GSD); Accra.

Ama Salah, I., Liégeois, J.-P., & Pouclet, A. (1996). Evolution d'un arc insulaire oceanique birimien pr´ecoce au Liptako nigérien (Sirba): Géologie, géochronologie et géochemie. *Journal of African Earth Sciences*, *22*, 235–254.

Amponsah, P. O., Salvi, S., Beziat, D., Baratoux, L., Siebenaller, L., Nude, P. M., … Jessell, M. W. (2015). The Bepkong deposit, Northwestern Ghana. *Ore Geology Reviews*, *78*, 718–723.

Amponsah, P. O., Salvi, S., Beziat, D., Baratoux, L., Siebenellar, L., Jessell, M., … Adubofour, E. G. (2016). Multistage gold mineralization in the Wa-Lawra greenstone belt, NW Ghana: The Bepkong deposit. *Journal of African Earth Science*, *120*, 220–237.

Anani, C. Y., Mahamuda, A., Kwayisi, D., & Asiedu, D. K. (2017). Provenance of sandstones from the neoproterozoic Bombouaka Group of the volta Basin, northeastern Ghana. *Arabian Journal of Geoscience*, *10*, 1–15.

Asiedu, D. K., Asong, S., Atta-Peters, D., Sakyi, P. A., Su, B.-X., Dampare, S. B., & Anani, C. Y. (2017). Geochemical and Nd-isotopic compositions of juvenile-type Paleoproterozoic Birimian sedimentary rocks from southeastern West African Craton (Ghana): Constraints on provenance and tectonic setting. *Precambrian Research*, *300*, 40–52.

Asiedu, D. K., Dampare, S., Asamoah-Sakyi, P., Banoeng-Yakubo, B., Osae, S., Nyarko, B. J. B., & Manu, J. (2004). Geochemistry of Paleoproterozoic metasedimentary rocks from the Birim diamondiferous field, southern Ghana: Implications for provenance and crustal evolution at the Archean-Proterozoic boundary. *Geochemical Journal*, *38*, 215–228.

Baratoux, L., Metelka, V., Naba, S., Jessell, M. W., Grégoire, M., & Ganne, J. (2011). Juvenile Paleoproterozoic crust evolution during the Eburnean orogeny (2.2–2.0 Ga), Western Burkina Faso. *Precambrian Research*, *191*, 18–45.

Béziat, D., Bourges, F., Debat, P., Lompo, M., Martin, F., & Tollon, F. (2000). A Paleoproterozoic ultramafic–Mafic assemblage and associated volcanic rocks of the Boromo greenstone belt: Fractionates originating from island-arc volcanic activity in the West African craton. *Precambrian Research*, *101*, 25–47.

Bhatia, M. R. (1983). Plate tectonics and geochemical composition of sandstones. *Journal of Geology*, *92*, 181–193.

Bhatia, M. R., & Crook, A. W. (1986). Trace element characteristics of greywackes and tectonic setting discrimination of sedimentary basins. *Contribution to Mineralogy and Petrology*, *92*, 181–193.

Blatt, H. G., Middleton, G. V., & Murray, R. C. (1980). *Origin of sedimentary rocks* (2nd ed.). Englewood cliff, N. J., Prentice Hall.

Block, S., Ganne, J., Baratoux, L., Zeh, L., Parra-Avila, A., Jessell, M., … Siebenaller, L. (2015). Petrological and geochronological constraints on lower crust exhumation during Paleoproterozoic (Eburnean) orogeny, NW Ghana, West African Craton. *Journal of Metamorphic Geology*, *33*, 463–494.

Boher, M., Abouchami, W., Michard, A., Albarède, F., & Arndt, N. T. (1992). Crustal growth in West Africa at 2.1 Ga. *Journal of Geophysical Research*, *97*, 345–369.

Bonhomme, M. (1962). Contribution à l'étude géochronologique de la plateforme de l'Ouest africain. In *Géologie et Minéralogie* (Vol. 5, pp.62). Gap: Impriemerie Louis-Jean, 1962..

Carney, J. N., Jordan, C. J., Thomas, C. W., Jordan, D. J., Kemp, S. J., & Duodo, J. A. (2010). Lithostratigraphy, sedimentation and evolution of the Volta Basin in Ghana. *Precambrian Research*, *183*, 701–724.

Condie, K. C. (1993). Chemical composition and evolution of the upper continental crust: Contrasting results from surface samples and shales. *Chemical Geology*, *104*, 1–37.

Crook, K. A. W. (1974). Lithogenesis and geotectonics: The significance of compositional variation in flysch arenites (greywackes). *Society of Economic Paleontology and Mineralogy Special Publication*, *19*, 304–310.

Dampare, S., Shibata, T., Asiedu, D., Okano, O., Manu, J., & Sakyi, P. (2009). Sr–Nd isotopic compositions of Paleoproterozoic metavolcanic rocks from the southern Ashanti volcanic belt, Ghana. Okayama University Earth Science Report 16, p. 9–28.

Davis, D. W., Hirdes, W., Schaltegger, U., & Nunoo, E. A. (1994). U–Pb constraints on deposition and provenance of Birimian and gold-bearing Tarkwaian sediments in Ghana, West Africa. *Precambrian Research*, *67*, 89–107.

De Kock, G. S., Theveniaut, H., Botha, P. W., & Gyapong, W. (2012). Timing the structural events in the Palaeoproterozoic Bole-Nangodi belt terrane and adjacent Maluwe basin, West African craton, in central-west Ghana. *Journal of African Earth Sciences*, *65*, 1–24.

Fedo, C. M., Eriksson, K. A., & Krogstad, E. J. (1996). *Geochemistry of shales from the Archean (3.0 Ga) Buhwa Greenstone Belt* (pp. 1751–1763). Zimbabwe: Implications for provenance and source area weathering. Geochimica Cosmochimica Acta 60.

Fedo, C. M., Nesbitt, H. W., & Young, G. (1995). Unraveling the effects of potassium metasomatism in sedimentary rocks and palaeosols, with implications for palaeoweathering conditions and provenance. *Journal of Geology*, *23*, 921–924.

Fedo, C. M., Young, G. M., & Nesbitt, H. W. (1997). Paleoclimatic control on the composition of the Paleoproterozoic Serpent formation, Huronian supergroup, Canada: A greenhouse to icehouse transition. *Precambrian Research*, *86*, 201–223.

Griffis, R. J., Barning, K., Agezo, F. L., & Akosah, F. K. (2002). *Gold deposits of Ghana* (pp. 438). Ghana: Minerals Commission, Accra.

Herron, M. M. (1988). Geochemical classification of terrigenous sands and shales from core or log data. *Journal of Sedimentary Petrology*, *58*, 820–829.

Hirdes, W., Davis, D. W., & Eisenlohr, B. N. (1992). Reassessment of Proterozoic granitoid ages in Ghana on the basis of U–Pb zircon and monazite dating. *Precambrian Researc*, *56*, 89–96.

Kalsbeek, F., Frei, D., & Affaton, P. (2008). Constraints on provenance, stratigraphic correlation and structural context of the Volta basin, Ghana, from detrital zircon geochronology: An Amazonian connection? *Sedimentary Geology*, *212*, 86–95.

Kasanzu, C., Makenya, M. A. H., & Manya, S. (2008). Geochemistry of fine-grained clastic sedimentary rocks of the Neoproterozoic Ikorongo Group, NE Tanzania: Implications for provenance and source rock weathering. *Precambrian Research*, *164*, 201–213.

Kesse, G. (1985). *The mineral and rocks resources of Ghana* (pp. 609). Boston: A.A. Balkema, Rotterdam.

Ledru, P., Pons, J., Milesi, J. P., Feybesse, J. L., & Johan, V. (1991). Transcurrent tectonics and polycyclic evolution in the lower proterozoic of Senegal-Mali. *Precambrian Research*, *50*, 337–354.

Leube, A., Hirdes, W., Mauer, R., & Kesse, G. O. (1990). The early proterozoic birimian supergroup of Ghana and some aspects of its associated gold mineralization. *Precambrian Research*, *46*, 139–165.

McLennan, S. M., Hemming, S., McDaniel, D. K., & Hanson, G. N. (1993). Geochemical approaches to sedimentation, provenance and tectonics. *Geological Society of America Special Paper*, *284*, 21–40.

McLennan, S. M., & Taylor, S. R. (1991). Sedimentary rocks and crustal evolution: Tectonic setting and secular trends. *Journal of Geology*, *99*, 1–21.

Nesbitt, H. W., Markovics, G., & Price, R. C. (1980). Chemical processes affecting alkalis and alkaline earths during continental weathering. *Geochimica et Cosmochimica Acta*, *44*, 1659–1666.

Nesbitt, H. W., & Young, G. M. (1982). Early Proterozoic climates and plate motions inferred from major element chemistry of lutites. *Nature*, *299*, 715–717.

Nesbitt, H. W., & Young, G. M. (1984). Prediction of some weathering trends of plutonic and volcanic rocks based on thermodynamic and kinetic considerations. *Geochimica Cosmochimica Acta*, *48*, 1523–1534.

Petersson, A., Scherstén, A., & Gerdes, A. (2018). Extensive reworking of Archaean crust within the Birimian terrane in Ghana as revealed by combined zircon U-Pb and Lu-Hf isotopes. *Geoscience Frontiers*, *9*, 173–189.

Pettijohn, F. J., Potter, P. E., & Siever, R. (1972). *Sand and sandstones*. New York, NY: Springer-Verlag.

Roddaz, M., Debat, P., & Nikiéma, S. (2007). Geochemistry of Upper Birimian sediments (major and trace elements and Nd–Sr isotopes) and implications for weathering and tectonic setting of the Late Paleoproterozoic crust. *Precambrian Research*, *159*, 197–211.

Rollinson, H. R. (1993). *Using Geochemical Data: Evaluation, Presentation, Interpretation* (pp. 352). New York, USA: Longman.

Roser, B. P., & Korsch, R. J. (1986). Determination of tectonic setting of sandstone–Mudstone suites using SiO_2 content and K_2O Na_2O ratio. *Journal of Geology*, *94*, 635–650.

Sakyi, P. A., Anum, S., Su, B.-X., Nude, P. M., Su, B.-C., Asiedu, D. K., … Kwayisi, D. (2018). Geochemical and Sr-Nd isotopic records of Paleoproterozoic metavolcanics and mafic intrusive rocks from the West African Craton: Evidence for petrogenesis and tectonic setting. *Geological Journal*, *53*, 725–741.

Sakyi, P. A., Su, B.-X., Anum, S., Kwayisi, D., Dampare, S. B., Anani, C. Y., & Nude, P. M. (2014). New zircon U-Pb ages for erratic emplacement of 2213–2130 Ma Paleoproterozoic calc-alkaline I-type granitoid rocks in the Lawra Volcanic Belt of Northwestern Ghana, West Africa. *Precambrian Research*, *254*, 149–168.

Samokhin, A. A., & Lashmanov, V. I. (1991). Geology and minerals of the northern part of the Bole Field Sheet, Ghana. Ghana Geological Survey Archive Report 53, p. 118.

Sylvester, P. J., & Attoh, K. (1992). Lithostratigraphy and composition of 2.1 Ga greenstone belts of the West African craton and their bearing on crustal evolution and Archean–Proterozoic boundary. *Journal of Geology*, *100*, 377–393.

Taylor, N. P., Moorbath, S., Leube, A., & Hirdes, W. (1992). Early Proterozoic crustal evolution in the Birimian of Ghana: Constraints from geochronology and isotope geochemistry. *Precambrian Research*, *56*, 97–111.

Taylor, S. R., & McLennan, S. M. (1985). *The continental crust: Its composition and evolution*. Oxford: Blackwell.

Vidal, M., & Alric, G. (1994). The Palaeoproterozoic (Birimian) of Haute-Comoé in the West African craton, Ivory Coast: A transtensional back-arc basin. *Precambrian Research*, *65*, 207–229.

Yang, H., Kyser, K., & Ansdell, K. (1998). Geochemical and Nd isotopic compositions of the metasedimentary rocks in the La Ronge Domain, Trans-Hudson Orogen, Canada: Implications for evolution of the domain. *Precambrian Research*, *92*, 37–64.